BULLETIN OF THE POLISH ACADEMY OF SCIENCES
TECHNICAL SCIENCES, Vol. 71(5), 2023, Article number: e147339
DOI: 10.24425/bpasts.2023.147339

Influence of plunger motion profile of high pressure die casting on the casting porosity and solidification rate

Katarzyna ŻAK[1]*, Rafał DAŃKO[1], Paweł L. ŻAK[1] and Wojciech KOWALCZYK[2]

[1] AGH University of Krakow, Faculty of Foundry Engineering, al. Mickiewicza 30, 30-059 Kraków, Poland
[2] Frech Poland Sp. z o.o., Przedmość, Główna 8, 46-320 Praszka, Poland

Abstract. The high pressure die casting (HPDC) is a technique that allows us to produce parts for various sectors of industry. It has a great application in such sectors as automotive, energy, medicine, as the HPDC allows us to produce parts very fast and very cheaply. The HPDC casting quality depends on many parameters. The parameters among others, are cast alloy alloy metallurgy, filling system design, casting technology elements geometry and orientation, as well as, machine operation settings. In the article, different plunger motion schemes of the HPDC machine were taken into account. Analyses lead to learning about plunger motion influence on the casting porosity and solidification process run. Numerical experiments were run with the use of MAGMASoft® simulation software. Experiments were performed for industrial casting of water pump for automotive. Main parameter taken into account was maximal velocity of the plunger in the second phase. The analysis covered porosity distribution, feeding time through the gate, temperature field during whole process, solidification time. Cooling curves of the casting in chosen points were also analysed. Obtained results allow us to formulate conclusions that connect plunger motion scheme, gate solidification time and the casting wall thickness on the solidification rate and porosity of the casting.

Key words: high-pressure die casting; computer simulation; cooling rate; numerical methods; aluminium alloy.

1. INTRODUCTION

The global die casting market is driven by its diverse application in such sectors of the economy as: automotive, energy, telecommunications etc. High-pressure die casting is one of the most cost-effective processes production used in the foundry industry. This process makes it possible to manufacture large light alloy parts with high precision and uniformity during mass production [1, 2].

For the casting plant customers the HPDC technique is understood, as the technique that gives high quality, uniform detail that is ready to use. Buyers of castings would like to have this idea in work. Casting companies have additional halls for post-production, which is necessary to have product that is wanted by the market. It is very difficult to design permanent mould for the HPDC machine that ensures high-quality product of the quality that is repeatable. However some solutions are well known, there cannot be directly utilized for new castings. There are many issues that have an impact on the HPDC product quality, which among others are: casting material, initial pouring temperature, heating/cooling of die (initial temperature at the beginning of the cycle), plunger motion scheme, design of the gating system and resulting filling rate of casting cavity volume, presence of vents [2–6].

*e-mail: kkz@agh.edu.pl

Manuscript submitted 2023-05-07, revised 2023-09-04, initially accepted for publication 2023-09-04, published in October 2023.

The HPDC technology is a complex process that depends on many parameters. Those are connected with piling up of the alloy in the shoot chamber, filling of the mould cavity and applying pressure on the edge of cooling system called biscuit [7–9].

Mentioned processes are driven by the three phases of the HPDC process. At the first stage of the process, filling of the shoot sleeve, and air evacuation from this volume happens. At the second stage of the process, mould cavity is being filled at the very high velocity. At the third stage of the process, intensification pressure is applied at the biscuit, which pushes liquid alloy into mould cavity through the gating system and gates, this alloy allows us to refill volumes empty due to the casting shrinkage. As the gates solidified no more feeding of the casting through the gates is possible, any hot-spots still present at this stage will result in shrinkage porosity of the final casting [2, 7, 8, 10, 11].

Despite that, a lot of research was done on the topic of elimination of shrinkage porosity, gas entrapment and other defects still it is a challenge to make optimal casting technology, just based on the casting geometry. That is why simulation is present in almost all HPDC foundries [2–4, 12]. Several simulation programs are used to optimize the HPDC technology, the most common used are: MAGMASoft® [13], FLOW 3D CAST [14], ProCAST, Nova Flow&Solid, AnyCasting [15, 16]. Mentioned programs use different numerical methods and different modelling methods. Simulation programs allow us to analyse different technology designs and their impact on the final product quality. Additional profit is understanding of process parame-

ters impact on its run without additional costs [17–19]. Workers who may analyse simulation results gets better qualification, as if they failed or succeeded during real production [20].

In order to support design of HPDC technology that will minimize casting defects, such as oxidation, air entrapment, shrinkage porosity several theoretical works were done. They use analytical formulas that allow us to choose best plunger motion schemes in the sense of minimizing the volume of entrapment air. As it was shown in [21,22] it was possible to model the free surface evolution and wave surface propagation in shot sleeve on the base of two-dimensional flow model based on shallow-water approximation. Analytical formulas for plunger motion rate and initial liquid level can help set process parameters.

The investigation reported in this manuscript is focused to asset the impact of plunger motion of HPDC machine on the parameters that define product quality after filling, solidification and cooling stage. Numerical experiments were performed with the use of MAGMASoft® 5.5 simulation system. The HPDC machine parameters were set in the programs dedicated module. It is well known that cooling rate and the alloy composition have great impact on the final casting microstructure [23–25].

2. MATERIALS AND METHODS

The aluminium-based EN AC – 46000 alloy (alloy chemical composition is given in Table 1) high pressure die casting (HPDC) was taken into account during investigation. This alloy is quite popular in the automotive industry as it allows to maintain high mechanical properties for thin-walled components. This alloy also has high fluidity, which allows us to fill even complicated shapes.

Table 1
Chemical composition of AlSi9Cu3 alloy

Element	Cu	Fe	Mg	Mn	Ni	Si	Zn	Al
Content [wt.%]	3.0	1.2	0.3	0.4	0.4	9.0	1.0	84.7

Chemical composition of EN AC – 46000 alloy has an impact on the thermophysical parameters of the material. These parameters are crucial in the case of heat flow in the casting volume. During numerical experiments standard MAGMASoft® database was used. Thermophysical data in this database depend on temperature, which have an impact on the process of filling, solidification and cooling during the HPDC process.

Several plunger motion profiles were taken into account. It was assumed to have standard formula (semi-scaled) plunger motion profiles – that assumption allows us to have comparable run of the process and the scaled velocity value can be used as an independent variable of the process. Within defined scheme some parameters are threatened as constants and some are dependent on the V_{MAX} value, which is only parameter that describes the plunger motion scheme. Plot visible in Fig. 1 can be also defined with Table 2, which defines plunger position and its velocity.

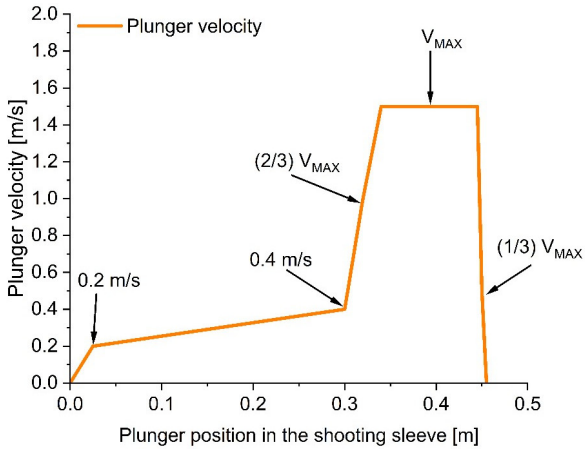

Fig. 1. The schematic of standardized run of plunger motion scheme depended on the maximal plunger velocity value V_{MAX}

Table 2
Values that define the run of plunger motion scheme

Plunger position [m]	Plunger velocity [m/s]
0	0
0.025	0.2
0.300	0.4
0.320	(2/3) V_{MAX}
0.340	V_{MAX}
0.445	V_{MAX}
0.450	(1/3) V_{MAX}
0.455	0

During the reported investigation seven values of the V_{MAX} were taken into account. Analysed values are gathered in Table 3. Intensification stage for all the cases was the same, with pressure of 210 bars.

Table 3
Maximal velocity of the plunger motion in the shot chamber of the HPDC machine

V_{MAX} [m/s]						
0.6	0.9	1.5	1.8	2.4	3.0	3.6

The examined casting was water pump cover, which is casted in four for per one HPDC cycle. Its geometry is shown in Fig. 2. The casting system and location of the casting nests are visible in Fig. 3.

The numerical modelling results were obtained with the use of MAGMASoft® 5.5.1 patch 5 simulation software. This program is complex software which allows us to examine different casting technologies. For the HPDC there is special module which allows us to simulate liquid alloy flow in a shot sleeve before and during first stage of HPDC process.

Fig. 2. Water pump cover geometry – view from MAGMASoft®

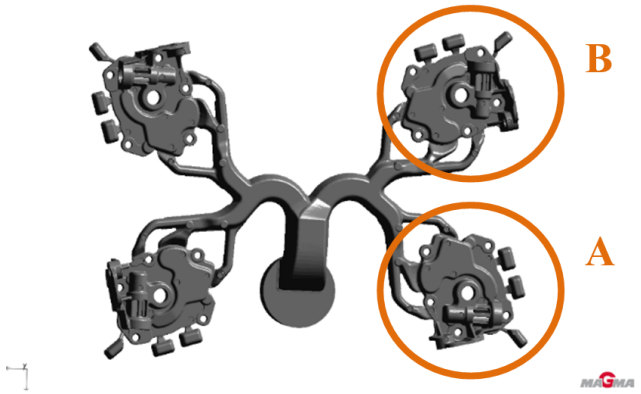

Fig. 3. The HPDC casting system for four water pump half-covers casted in one HPDC shoot

At the analysis stage standard and user-defined results were taken into account. Standard results were to compare visual in the general or clipped view, to understand fluid flow: rate, first filled gate, air entrapment, also to understand local temperature or porosity distribution. As a user-defined result it was chosen to use integrals of the porosity in the mesh cells of the casting volume. Software result "porosity" shows percentage fraction of the void in each cell. Sum of porosity value over the cavity cells is comparable result as during each numerical experiment same mesh was used. Number of cartesian elements for discretization of each casting was about 600 000 cells, about 220 000 cells for gating system discretization. In both dies volume almost 35 million of cartesian cells was generated, which after coarsening process were reduced to about 7 200 000 cells. In the Integral of porosity was done for total casting volume and for each individual casting.

During simulations virtual thermocouples were placed in the casting volumes and nearby permanent mould. They were placed at the regions where characteristic 3, 6, 11 mm wall thickness was measured, Fig. 2. Cooling curves can give a lot of useful information about process run and its characteristic stages. Simulation software allows us to obtain temperature curves for geometries that were first marked as individual domains, i.e. gates, individual castings. These curves cover temperature history, flow rate through the domain volume and others. Another "user" result was the time of gate solidification, which has large impact on the feeding of the casting volume which is needed due to alloy shrinkage.

3. RESULTS AND DISCUSSION

Following paragraph presents results that was obtained during simulation.

In Figs. 4, 5 porosity distribution within casting A (Fig. 4) and casting B (Fig. 5) are shown. It can be clearly seen that in the case of greater velocities, V_{MAX}, larger porosity regions appears in the casting. Results visible in mentioned Figs. 4, 5 – blue regions – can be assessed by the shape and size of porosity region volume. Because of the growth of the porosity fraction in the porosity regions visual analysis maybe misleading. That is why in Table 4 weighted integral of porosity volume for all four casting in total is gathered. Those results connected with V_{MAX} clearly confirm tendency that was observed in Figs. 4, 5.

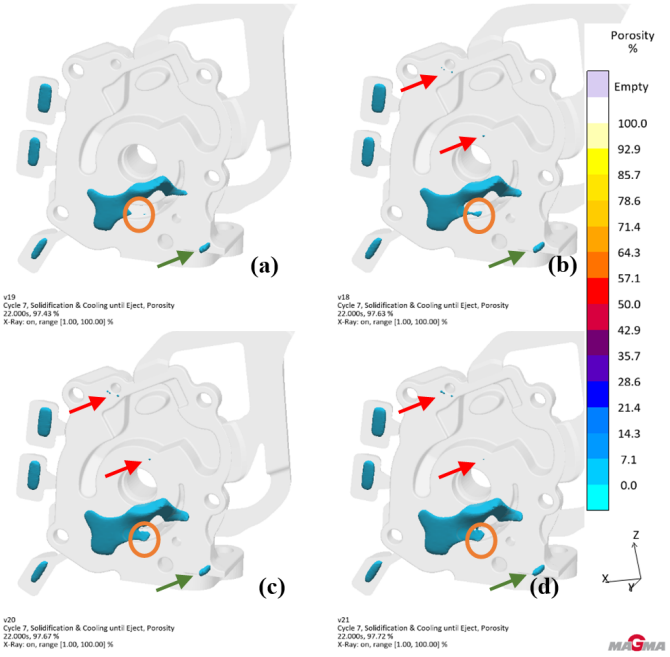

Fig. 4. Forecasted porosity distribution for different piston speeds in the bottom A, casting: V_{MAX} = 0.9 [m/s] (a), V_{MAX} = 1.8 [m/s] (b), V_{MAX} = 2.4 [m/s] (c), V_{MAX} = 3.6 [m/s] (d)

Table 4
Comparison of the predicted porosity dependence on the V_{MAX}

V_{MAX} [m/s]	Porosity volume [–]
0.6	19.9
0.9	25.2
1.5	29.8
1.8	30.3
2.4	32.9
3.0	33.9
3.6	34.3

Porosity regions visible in Figs. 4, 5 are different, not only for the V_{MAX} change, but for the same velocity and different A and B castings. Distribution of the porosity in the bottom A

(Fig. 4) and the top B casting (Fig. 5) differs significantly. In the Fig. 4a–d central porosity region can be observed as two connected regions: one is larger, second smaller (denoted with orange circle). In Fig. 4b this small region (orange circle) is larger and is connected to larger, central porosity region. As V_{MAX} value grows, Figs. 4c–d, evolution of this central region size and shape can be seen. Volume of the central porosity changes and become larger. Other defects that are visible in Fig. 4a (denoted green arrows) are not evolving so much in shape, however new small regions appears, which may be located in Figs. 4b–d (denoted red arrows). In Fig. 5a large isolated porosity region is centre-located, similarly as in Fig. 4a. However, this region is smaller than centre-located region in casting A, Fig. 4. The small spherical region also can be visible near to this region, but its location is different than in Fig. 4a. Small region of porosity is located more to the centre of the casting (denoted green circle). In following Figs. 4b–c this region is growing and is a part of largest porosity region. As the V_{MAX} equals 1.8 [m/s], Fig. 5b, new small spherical region appears (denoted with orange circle). It is located in the similar place as it was in Fig. 4a. Its behaviour is similar as region denoted with orange circle in Fig. 4. For the higher V_{MAX}, Fig. 5c, d large porosity region is connected with this small porosity also and creates one porosity region. In the case of casting B no new, far regions of porosity appears in the casting, Figs. 5a–d.

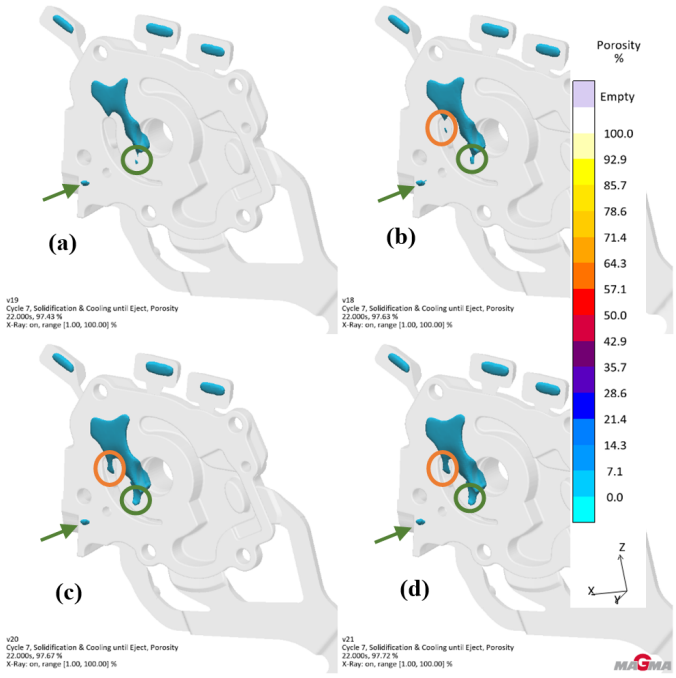

Fig. 5. Forecasted porosity distribution for different piston speeds in the top, B, casting: V_{MAX} = 0.9 [m/s] (a), V_{MAX} = 1.8 [m/s] (b), V_{MAX} = 2.4 [m/s] (c) and V_{MAX} = 3.6 [m/s] (d)

Quantity result of weighted integral volume of porosity for casting A and B are gathered in Table 5. In this case only several V_{MAX} values are present. Results show tendency that connects porosity volume and V_{MAX}. It can be observed that total porosity in casting A is larger than for casting B for each V_{MAX}. Based on the obtained results it can be said that porosity volume grows faster for the casting A. However no strict tendency can be noted. Results from Table 5 confirms results that were from Figs. 4, 5 and Table 4. It can be also noted that position of the casting, filling gate placement and shape of the filling system has an impact on the porosity. It is also seen that different gravity direction during the solidification would have impact on the casting porosity location and size. However from mentioned parameters the V_{MAX} value has most significant impact on the casting quality. According to the obtained results it is possible to connect a variety of different parameters to gain best casting quality.

Table 5
Comparison of the predicted porosity dependence on the V_{MAX} for chosen castings volumes

V_{MAX} [m/s]	Porosity volume [mm^3]	
	Casting A	Casting B
0.6	3.461	2.997
0.9	4.295	3.691
1.8	5.187	4.425
2.4	6.647	5.545
3.6	6.922	5.672

To understand the porosity change with the V_{MAX} some additional measurements were made. Using special defined "user result" it was possible to identify the maximal feeding time through the casting cavity gate, Fig. 6 and porosity in specified casting, Fig. 7. The region of the longest feeding time was always located in the largest of three gates through which casting was filled. In many simulation programs, no full physical feeding model is used. Programs use critical volume of dendrites that make it impossible for liquid to travel through their arms. Same feature is not used anymore by MAGMASoft®, and new approach, based on Darcy's law, is applied. In the presented results limit time was chosen at the stage when software stopped

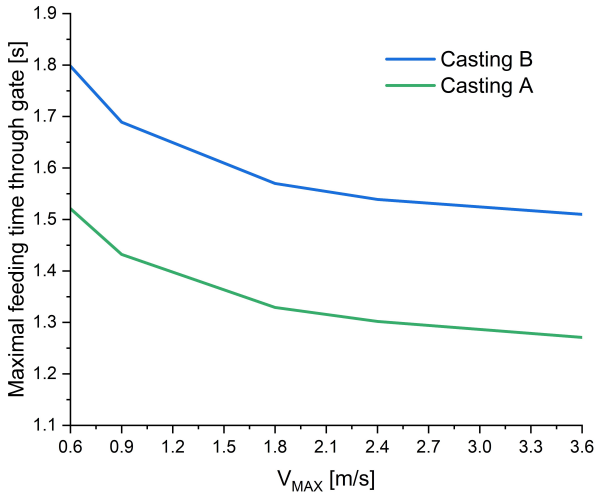

Fig. 6. Change of the feeding time with the maximal plunger velocity

transfer of liquid through the gate, and limiting start of filling was registered at the time when the cavity is fully filled. Obtained results clearly show that if the gate can longer transfer the liquid alloy the resulting casting porosity is lower.

Results shown in Figs. 6 and 7 in a form of the plots allow us to observe, that there is connection between feeding time from the filling system and total porosity volume values. However there are some differences visible in the run of maximal feeding time vs. V_{MAX} and porosity volume vs. V_{MAX}, general statement about their dependency may be made. For a longer feeding time porosity volume would be smaller.

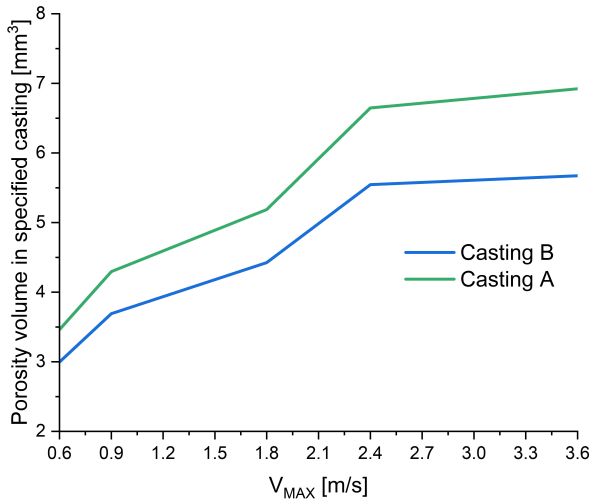

Fig. 7. Change of the porosity volume in whole casting with the maximal plunger velocity

After stabilization of the temperature field in the cover and ejector die during filling, different amount of energy is transferred into the die volume. It strictly depends on mould cavity filling time. With different V_{MAX} values different temperature profiles in the casting volumes are obtained. The results are shown in Fig. 8. Scale bar is the same for all castings and covers liquidus temperature to pouring temperature range, which allows us to compare coloured maps. All visible regions are still at temperature above liquidus temperature, and total casting volume is full of liquid alloy. In the case of the fresh filled casting the lowest temperature is on their surface. As for V_{MAX} = 0.9 m/s there are large regions of temperature about 600°C at the higher values of V_{MAX} temperatures are much higher. For V_{MAX} equal to 1.8 m/s the lowest temperature is still higher than 630°C. The highest examined V_{MAX} velocity 3.6 m/s the temperature distribution map shows that temperature is almost equally distributed and differs in range 650–670°C.

With different plunger motion velocities filling time of the cavity varies in the range 128–30 ms for V_{MAX} values in the range 0.9–3.6 m/s (see Table 7). During filling of the die cavity stage liquid alloy contact area with ejector and cover die grows and energy transfer from alloy to die is possible. Mentioned contact time is longer for lower V_{MAX} so more energy can be transferred from liquid alloy to the permanent mould. This phenomenon impacts not only alloy temperature distribution in mould cavity but also temperature distribution in die around the casting. Presented results take into account cycling of the HPDC process and are given for third production cycle.

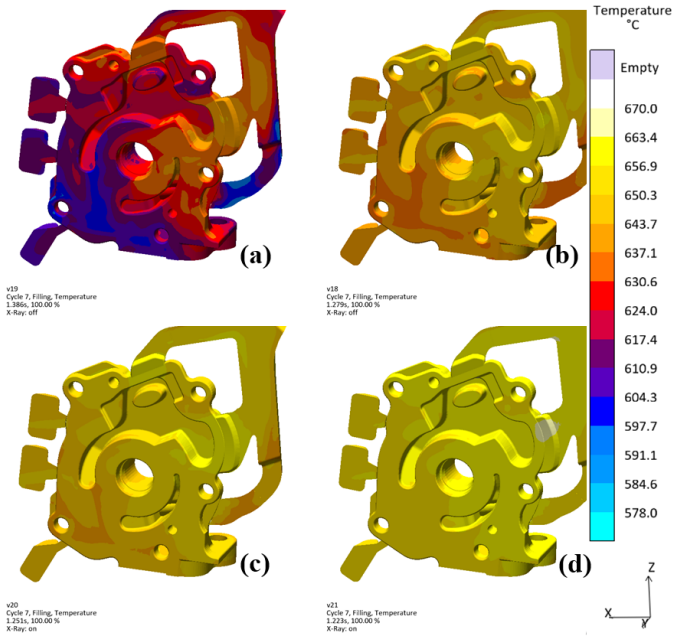

Fig. 8. Temperature field in the end of filling in the first production cycle: V_{MAX} = 0.9 [m/s] (a), V_{MAX} = 1.8 [m/s] (b), V_{MAX} = 2.4 [m/s] (c) and V_{MAX} = 3.6 [m/s] (d)

During the examination three regions of different wall thickness of the casting, Fig. 1, were chosen. Near virtual thermocouples placed in the middle of the cavity, 4 mm from the casting edge additional thermocouples were placed in ejector die. Those thermocouples constantly registered temperature change during process, their placement is denoted with red arrows in Fig. 9. Its run differs significantly for different plunger velocities, to reach different maximal temperature at the end of the filling of the casting cavity stage. Registered values are gathered in Table 6. It can be noted that in each thermocouple temperature value versus V_{MAX} tendency is similar – for higher velocities temperature of die gets lower. As the filling time is longer the temperature of die is higher which results in lower alloy temperature and higher permanent mould temperature. Percentage reduction of temperature value is the greatest for the wall of 3 mm thickness (about 24%). For other wall thicknesses per-

Table 6
Maximal temperatures at the end of the casting cavity filling, measured in ejector die 4 mm from the casting wall near given wall thickness of the casting A

V_{MAX} [m/s]	0.9	1.8	2.4	3.6
Wall thickness [mm]	Temperature °C			
3	105.95	88.03	84.25	79.39
6	202.12	179.53	172.34	165.54
11	211.47	184.22	178.31	170.22

centage reduction of temperature is less (about 18–19%) but still appears as significant observation. As a result temperature gradient between casting and die is smaller for smaller V_{MAX} values. At the filling stage all heat energy is transferred into system, so it is very important to understand how it will be distributed. As the flow is slower more time is given for the alloy to heat up the neighbourhood die regions. After this stage the storage energy will allow for slower solidification as well as longer feeding from the casting filling system gate. At the solidification stage the only source of casting cavity feeding material is biscuit and filling system due to pressure from plunger at the pressure intensification stage.

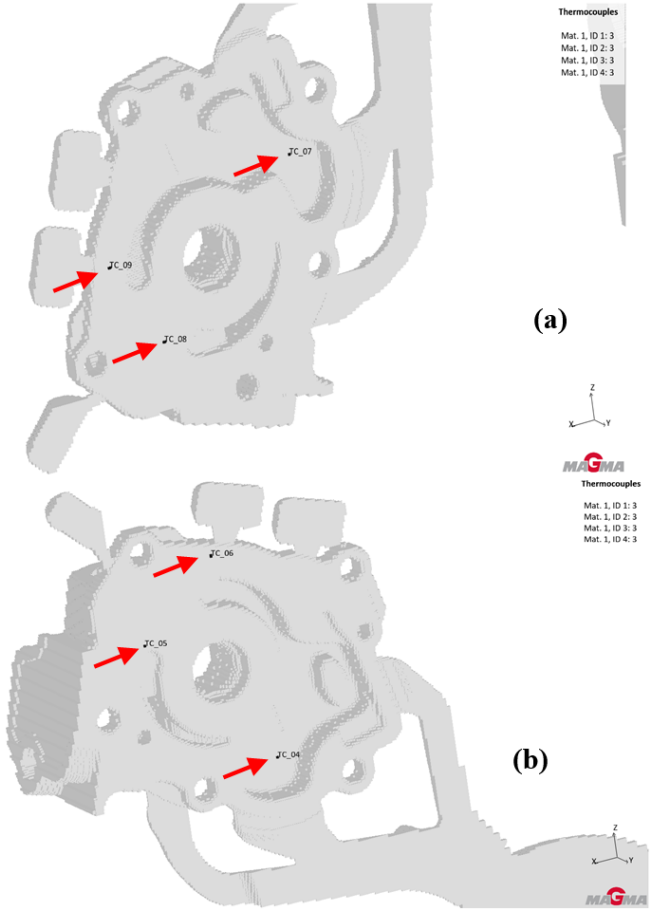

Fig. 9. Placements of the virtual thermocouples – view on the computational mesh. (a) A casting, (b) B casting. Thermocouples are indicated by red arrows

During each analysis, V_{MAX} – depended, plunger motion scheme filling time is quite short in comparison with whole HPDC process, however small differences have significant effect on resulting temperatures, compare Table 6 and Fig. 8. For the casting cavity volume longer filling time will result in lower temperatures of the liquid alloy. For the die volume, near to the casting, longer filling time will result in the higher temperature. Sum of those effects will result in lower temperature gradient between casting cavity and permanent mould for lower plunger motion speed and higher temperature gradient for faster maximal plunger motion speed.

Analysis of the solidification time for representative casting A was also done. Its results are shown in Table 8 and the cooling curves presented in Fig. 10. Data was gathered from the wall of 11 mm thickness. It can be seen that differences for values gathered in Table 8 as well as run of the cooling curve Fig. 10 are not significant. For the lowest plunger velocity solidification time is the shortest (just above 4.9 s), and for the fastest plunger velocity solidification time is longest (over 5 seconds). Analysis of the time change trend show slow growth, however statistical correlation for this approximation is less than 50%. Taking into account small relative differences it can be assumed that solidification time is almost the same for all V_{MAX} values.

Table 7

Start and end of the filling of the mould cavity related to the moment of beginning of the plunger motion – values for casting A

V_{MAX} [m/s]	Start of filling [ms]	End of filling [ms]	Filling time [ms]
0.6	1295	1489	194
0.9	1258	1386	128
1.8	1218	1279	61
2.4	1206	1251	45
3.6	1193	1223	30

Table 8

Solidification times of the A – casting in the centre of 11 mm wall – for different maximal plunger motion speeds

V_{MAX} [m/s]	Solidification time [ms]
0.6	4914
0.9	4949
1.5	4945
1.8	4898
2.4	4984
3.0	4987
3.6	5039

The obtained result can be explained by different temperature gradient between casting and die volume at the end of cavity filling stage. Previously registered values show that for slower V_{MAX} much more energy was transferred from liquid alloy to the die at filling stage, which has an effect in the liquid metal average temperature and higher die temperature. It is well known that temperature gradient value is proportional to cooling rate. In this case at the filling stage large portions of energy were transferred from casting to permanent mould volume. It is due to pouring new volumes of liquid transferred by the biscuit and runner because of plunger motion. However, when filling stage finishes energy value gathered in the system (casting cavity volume and die) remains constant. As temperature values evolve slower – no metal flow – main effect on the heat transfer

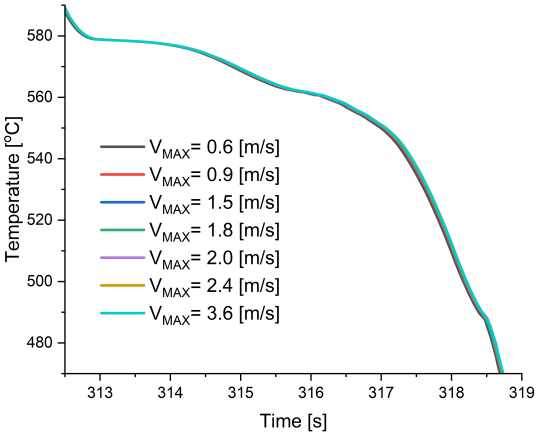

Fig. 10. Cooling curves of the casting A during solidification for different values of V_{MAX} (denoted v in the plot)

would have the temperature gradient. For larger V_{MAX} values, temperature gradient is much greater than for low filling velocities. This effect counterbalance previous observed temperature – plunger velocity relations. At the end of mould cavity filling stage (high V_{MAX}), average temperature of liquid alloy is large in comparison with die temperature. In effect much larger temperature gradient than for lower V_{MAX} is observed. During filling stage for slower V_{MAX} much more energy was transferred from alloy to die. Now, at the solidification stage smooth temperature change between casting cavity volume and the die makes temperature gradient much lower and the energy transfer is slow in comparison with the fast V_{MAX}.

4. CONCLUSIONS

Presented results and discussion enable us to state following conclusions.

Numerical simulation allows us to predict run of the HPDC process, including machine preparation, filling of the mould cavity, solidification, cooling, pressure application and removing casting from die phenomena. Thiese advanced tools allow us to analyse the impact of the plunger motion scheme on the casting quality.

Casting quality control is possible by change of HPDC machine parameters. Modelling of those parameters is possible with simulation software. Simulation software allows us to understand run of the process and parameters which are crucial for it.

Location of the casting has an impact on the casting quality. Analysed cases show that casting which is higher in die has better quality than the lower one. It, however, is not effect of the gravity – nowadays research shows, that HPDC process is so fast, that gravity impact may be neglected. In this case main impact on the casting quality have design of the filling system. As different casting filling systems are used different casting filling runs are obtained, as well as different temperature profiles.

Change of the plunger motion scheme value V_{MAX}, has an impact on the porosity volume in the casting. For higher velocities greater porosity volume in the casting is observed, regions of porosity appearance are also significantly larger.

During research it was shown that larger porosity for higher velocities is connected to following factors:

- temperature of the die at the end of the filling process the casting cavity is smaller for higher V_{MAX}, on the other hand liquid metal temperature value is greater, it is caused by differences in the filling time and possibility of energy transfer from liquid to die,
- large gradient of temperature makes it faster to solidify gate volume, which makes gate feeding time shorter. The longer gate feeding time, the less porosity can be observed in the casting volume.

Solidification time of the casting depends on wall thickness. Due to temperature gradient between liquid and permanent mould very small differences in solidification time were noted for V_{MAX} ranged 0.6–3.6 m/s, in the centre of 11 mm thick wall.

ACKNOWLEDGEMENTS

This research was supported by AGH project no 16.16.170. 7998/B307.

REFERENCES

[1] M. Łuszczak and R. Dańko, "The state of art of production of automotive structural die casted elemenets," *Arch. Foundry Eng.*, vol.13, no. 3–Special Issue, 2013.

[2] S. Devaraj, G. Veeresh, and I. Siddhalingeshwar, "Review on state of the art and techniques in high pressure die-casting (HPDC)," *Int. J. Sci. Eng. Res.*, vol. 9, pp. 60–68, 2018.

[3] C. Ammen, *Metalcasting*. McGraw Hill Professional, 2000.

[4] H. Cao, Z. Luo, C. Wang, J. Wang, T. Hu, L. Xiao, and J. Che, "The stress concentration mechanism of pores affecting the tensile properties in vacuum die casting metals," *Materials*, vol. 13, no. 13, p. 3019, 2020, doi: 10.3390/ma13133019.

[5] E. Fiorese, D. Richiedei, and F. Bonollo, "Improving the quality of die castings through optimal plunger motion planning: analytical computation and experimental validation," *Int. J. Adv. Manuf. Technol.*, vol. 88, no. 5, pp. 1475–1484, Feb 2017, doi: 10.1007/s00170-016-8875-y.

[6] R. Dańko and W. Kowalczyk, "New trends in cold-chamber die casting machine design." *China Foundry*, vol. 12, no. 4, pp. 305–309, 2015.

[7] A.R. Adamane, L. Arnberg, E. Fiorese, G. Timelli, and F. Bonollo, "Influence of injection parameters on the porosity and tensile properties of high-pressure die cast Al-Si alloys: A review," *Int. J. Met.*, vol. 9, pp. 43–53, 2015, doi: 10.1007/BF03355601.

[8] W. Kowalczyk, R. Dańko, M. Górny, M. Kawalec, and A. Burbelko, "Influence of high-pressure die casting parameters on the cooling rate and the structure of EN-AC 46000 alloy," *Materials*, vol. 15, no. 16, p. 5702, 2022, doi: 10.3390/ma15165702.

[9] Q. Han and J. Zhang, "Fluidity of alloys under high-pressure die casting conditions: Flow-choking mechanisms," *Metall. Mater. Trans. B-Proc. Metall. Mater. Proc. Sci.*, vol. 51, no. 4, pp. 1795–1804, Aug 2020, doi: 10.1007/s11663-020-01858-0.

[10] J. Zheng, Q. Wang, P. Zhao, and C. Wu, "Optimization of high-pressure die-casting process parameters using artificial neural network," *Int. J. Adv. Manuf. Technol.*, vol. 44, no. 7, pp. 667–674, Oct 2009, doi: 10.1007/s00170-008-1886-6.

[11] F. Bonollo, N. Gramegna, and G. Timelli, "High-pressure die-casting: Contradictions and challenges," *JOM*, vol. 67, no. 5, pp. 901–908, May 2015, doi: 10.1007/s11837-015-1333-8.

[12] L. Wang, P. Turnley, and G. Savage, "Gas content in high pressure die castings," *J. Mater. Process. Technol.*, vol. 211, no. 9, pp. 1510–1515, 2011, doi: 10.1016/j.jmatprotec.2011.03.024.

[13] MAGMASoft®, *MAGMASoft® manual and database version 5.5.1.5*, Aahen, Germany, 2023. [Online]. Available: https://www.magmasoft.de/en/

[14] I. Flow Science, *FLOW-3D, Version 2023R1*, Santa Fe, NM, USA, 2023. [Online]. Available: https://www.flow3d.com/

[15] K. Dou, E. Lordan, Y. Zhang, A. Jacot, and Z. Fan, "A complete computer aided engineering (cae) modelling and optimization of high pressure die casting (hpdc) process," *J. Manuf. Process.*, vol. 60, pp. 435–446, 2020, doi: 10.1016/j.jmapro.2020.10.062.

[16] H.-J. Kwon and H.-K. Kwon, "Computer aided engineering (cae) simulation for the design optimization of gate system on high pressure die casting (hpdc) process," *Robot. Comput.-Integr. Manuf.*, vol. 55, pp. 147–153, 2019, extended Papers Selected from FAIM2016.

[17] A.R. Jadhav, D.P. Hujare, and P.P. Hujare, "Design and optimization of gating system, modification of cooling system position and flow simulation for cold chamber high pressure die casting machine," *Mater. Today-Proc.*, vol. 46, pp. 7175–7181, 2021, 3rd International Conference on Materials, Manufacturing and Modelling.

[18] T. Wang, J. Huang, H. Fu, K. Yu, and S. Yao, "Influence of process parameters on filling and feeding capacity during high-pressure die-casting process," *Appl. Sci.*, vol. 12, no. 9, p. 4757, 2022, doi: 10.3390/app12094757.

[19] M.E. Mehtedi, T. Mancia, P. Buonadonna, L. Guzzini, E. Santini, and A. Forcellese, "Design optimization of gate system on high pressure die casting of AlSi13Fe alloy by means of finite element simulations," 2020, vol. 88, pp. 509–514, doi: 10.1016/j.procir.2020.05.088.

[20] J. Martínez-Pastor, J.J. Hernández-Ortega, and R. Zamora, "A decision support system (DSS) for the prediction and selection of optimum operational parameters in pressure die-casting processes," *Materials*, vol. 15, no. 15, p. 5309, 2022, doi: 10.3390/ma15155309.

[21] F. Faura, J. López, and J. Hernández, "On the optimum plunger acceleration law in the slow shot phase of pressure die casting machines," *Int. J. Mach. Tools Manuf.*, vol. 41, no. 2, pp. 173–191, 2001, doi: 10.1016/S0890-6955(00)00079-1.

[22] J. Lo´pez, F. Faura, J. Herna´ndez, and P. Go´mez, "On the Critical Plunger Speed and Three-Dimensional Effects in High-Pressure Die Casting Injection Chambers ," *J. Manuf. Sci. Eng.-Trans. ASME*, vol. 125, no. 3, pp. 529–537, 07 2003, doi: 10.1115/1.1580525.

[23] F. Grosselle, G. Timelli, F. Bonollo, and E. Della Corte, "Correlation between microstructure and mechanical properties of Al-Si cast alloys," *Metall. Ital.*

[24] J.G. Kaufman and E.L. Rooy, *Aluminum alloy castings: properties, processes, and applications*. Asm International, 2004.

[25] S.G. Shabestari and F. Shahri, "Influence of modification, solidification conditions and heat treatment on the microstructure and mechanical properties of A356 aluminum alloy," *J. Mater. Sci.*, vol. 39, no. 6, pp. 2023–2032, Mar 2004, doi: 10.1023/B:JMSC.0000017764.20609.0d.